A labeling intercomparison of retrogressive thaw slumps by a diverse group of domain experts

I.Nitze[1], J.Van der Sluijs[2], S.Barth[1,3,4], P.Bernhard[5], L.Huang[6], M.J.Lara[7], A.Kizyakov[8], N.Nesterova[1, 3], A.Runge[9,1], A.Veremeeva[1], M.Ward Jones[10], C.Witharana[11], Z.Xia[12,7], A.K. Liljedahl[13]

Affiliations

1 Alfred Wegener Institute, Permafrost research section, Potsdam, Germany, ingmar.nitze@awi.de, sophia.barth@awi.de, nina.nesterova@awi.de, aleksandra.veremeeva@awi.de

2 NWT Centre for Geomatics, Government of Northwest Territories, Yellowknife, Canada, jurjen_vandersluijs@gov.nt.ca.

3 University of Potsdam, Institute of Geoscience, Potsdam, Germany

4 Joint Research Center, Ispra, Italy

5 Department of Civil Environmental and Geomatic Engineering, ETH Zurich, Switzerland, bernhard@ifu.baug.ethz.ch.

6 Institute of Space and Earth Information Science, The Chinese University of Hong Kong, Shatin, N.T., Hong Kong SAR, China, lingcaohuang@cuhk.edu.hk.

7 Department of Plant Biology, University of Illinois at Urbana-Champaign, Urbana, Illinois, USA; Department of Geography, University of Illinois at Urbana-Champaign, Urbana, Illinois, USA, mjlara@illinois.edu.

8 Lomonosov Moscow State University, Department of Cryolithology and Glaciology, Faculty of Geography, Moscow, Russia, akizyakov@mail.ru.

9 GFZ German Research Centre for Geosciences, Remote Sensing and Geoinformatics, Potsdam, Germany alexandra.runge@gfz-potsdam.de.

10 Water and Environmental Research Center (WERC), University of Alaska Fairbanks, PO Box 755910, Fairbanks, AK 99775-5910, mkwardjones@alaska.edu.

11 Department of Natural Resources and the Environment, University of Connecticut, Storrs, CT 06269, USA, chandi.witharana@uconn.edu.

12 Earth System Science Programme, Faculty of Science, The Chinese University of Hong Kong, Hong Kong SAR, China, ZhuoxuanXIA@link.cuhk.edu.hk.

13 Woodwell Climate Research Center, 149 Woods Hole Road, Falmouth 02540-1644, MA, United States, aliljedahl@woodwellclimate.org.

This is a non-peer reviewed version submitted to EarthArXiv. This manuscript was submitted for peer-review to Permafrost and Periglacial Processes.

Highlights

- Labeling experiment of retrogressive thaw slumps by a group of international domain experts
- Noticeable variation between domain experts and study sites
- Variation driven by regional knowledge and scientific objective of experts
- Common guidelines highly recommended to achieve higher consensus

Abstract

Deep-learning (DL) models have become increasingly beneficial for the detection of retrogressive thaw slumps (RTS) in the permafrost domain. However, comparing accuracy metrics is challenging due to unstandardized labeling guidelines. To address this, we conducted an experiment with 12 international domain experts from a broad range of scientific backgrounds. Using 3m PlanetScope multispectral imagery, they digitized RTS footprints in two sites. We evaluated label uncertainty by comparing manually outlined RTS labels using Intersection-over-Union (IoU) and F1 metrics. At the Canadian Peel Plateau site, we see good agreement, particularly in the active parts of RTS. Differences were observed in the interpretation of the debris tongue and the stable vegetated sections of RTS. At the Russian Bykovsky site, we observed a larger mismatch. Here, the same differences were documented, but several participants mistakenly identified non-RTS features. This emphasizes the importance of site-specific knowledge for reliable label creation. The experiment highlights the need for standardized labeling procedures and definition of their scientific purpose. The most similar expert labels outperformed the accuracy metrics reported in the literature, highlighting human labeling capabilities with proper training, site knowledge, and clear guidelines. These findings lay the groundwork for DL-based RTS monitoring in the pan-Arctic.

Keywords: retrogressive thaw slumps, deep learning, remote sensing, uncertainty estimation, permafrost, hillslope thermokarst

Introduction

The northern high latitudes are affected by a rapidly changing climate (Chylek et al., 2022; Serreze & Barry, 2011) with further warming and wetting expected over the coming decades (Meredith et al., 2019). This will have an impact on vulnerable permafrost landscapes, with a potential increase in permafrost thaw and degradation. Many regions with ice-rich ground are already affected by hillslope thermokarst, such as retrogressive thaw slumps (RTS). RTS are dynamic geomorphological mass-wasting features prevalent across ground-ice-rich permafrost regions around the Arctic and Qinghai-Tibetan Plateau. The landform is triggered by thawing and collapsing ice-rich ground, which continues to propagate upslope via the process of ice ablation (Burn & Lewkowicz, 1990). RTS are typically confined to regions with ice-rich permafrost. RTS as a geomorphological feature, contain distinct parts, such as a headwall, scar zone, and debris tongue (Fig 1). Their size can range from a few m^2 to approximately two km^2. They are temporally variable and often exhibit polycyclic (i.e., recurring over time) dynamics (Kerfoot, 1969; Mackay, 1966), which are influenced by weather, climate, and local geomorphological conditions. In most cases they are located close to water bodies, such as rivers, sea coasts or lake shores, as well as dynamic morphological gradients, such as valleys and slopes. In their immediate vicinity and in downstream environments they can have a strong impact on hydrology, geomorphology, and various biogeochemical cycles (Kokelj et al., 2021). With drastically changing climate in the arctic and high-mountain regions, RTS dynamics have rapidly accelerated over the past decades as determined through manual mapping approaches (Lantz & Kokelj, 2008; Segal et al., 2016; Van Der Sluijs et al., 2023; Ward Jones et al., 2019).

Conventional mapping initiatives for RTS rely heavily on manual mapping and detailed local geomorphological knowledge and/or semi-automated mapping approaches (Kokelj et al., 2017, 2021; Lantz & Kokelj, 2008; Lewkowicz & Way, 2019; Mackay, 1966; Swanson & Nolan, 2018). The science community have just begun to produce pan-Arctic datasets of mapped RTS (Huang et al., 2023) as more automated, machine-learning (ML) or deep learning (DL) based approaches have become popular over the past decade (Nitze et al., 2018; Runge et al., 2022). In combination with large improvements in the availability of satellite imagery (Wulder et al., 2022) and computational power, such as cloud- or high performance computing, fine-resolution large-domain products are now possible. Typically, most DL workflows are supervised approaches, requiring a high quantity and quality of manually produced training labels (Rädsch et al., 2023). However, the availability and usability of labels acquired across various spatial, spectral, and temporal scales is still limited as of now. Therefore, manual labeling has often been used to increase the number of training labels in DL applications. As many labels are required (preferably in the thousands), distributing this work within a team or even across an entire science community becomes an important and necessary step for scaling. To support effective community-wide label synthesis, clear definitions and guidelines on how to label target features are required. In addition, efforts to evaluate the label variability among analysts will be critical to maintain data quality and consistency (Plank, 2022). While anthropogenic objects, such as buildings or airplanes have distinct and clear boundaries and well-understood ontologies, natural object boundaries are much more variable and often ambiguous or dependent on the particular use case and definition. Particularly labeling dynamic geomorphological features that initiate and expand over time, such as RTS, is often challenging due to variable atmospheric (i.e. haze, clouds, smoke) and environmental conditions (i.e. plant pheno-period and soil moisture availability). Beyond these externally changing conditions, inherent RTS processes during initiation (e.g vegetation removal and exposure of bare earth), growth (e.g mud slurries, expanding boundaries), and stabilization (revegetation) means that a RTS as a landform can appear very differently through time, affecting its abstract representation and consistency of DL labeling efforts.

With the increasing popularity of DL (Ma et al., 2019; Zhu et al., 2017), label availability and quality becomes an increasingly important topic. Over the past decades the permafrost and RTS research community has increased in diversity from a traditional earth science and geomorphology people to a broader group, with different domain backgrounds such as ecology, remote sensing, and computer science. Experience in field work has also diversified, which may influence labeling consistency and quality. Thus, the scope of RTS research has also broadened to more diverse objectives and analyses such as large-scale mapping, change detection, and environmental impacts, which may lead to different definitions or classifications of which parts belong to an RTS.

Recent DL initiatives for mapping RTS across different locations within the permafrost extent, such as Siberia (Yang et al., 2023), Tibetan Plateau (Huang et al., 2020, 2021; Xia et al., 2022), Northern Canada (Witharana et al., 2022), various localities across the Arctic (Nitze et al., 2021), or the entire Arctic (Huang et al., 2023), used different methods and imagery sources, to train and validate their models. For example, (Huang et al., 2020, 2021; Nitze et al., 2021; Witharana et al., 2022; Xia et al., 2022) created their own hand-drawn labels, while (Yang et al., 2023) used a combination of newly hand-drawn labels and already existing external sources e.g. (Nitze et al., 2021). However, they all achieved accuracy metrics using IoU (intersection over Union), which ranged from low to very good agreement: 0.15-0.58 (Nitze et al., 2021), 0.71-0.74 (Yang et al., 2023) or F1 of 0.25-0.73 (Nitze et al., 2021), 0.85 (Huang et al.,

2020) and 0.75-0.85 (Witharana et al., 2022). As these values are relative to validation data based on self-created hand-drawn labels, and not independent benchmark datasets, accuracy metrics are difficult to compare across methods and geographical regions. Using different image sources further complicates the comparison of the different studies. Furthermore, sampling strategies (e.g. grid, random, stratified, manual) exacerbate the difficulties of comparing RTS segmentation studies as landscapes produce a wide variety of RTS expressions due to differing topographical, sub-surface, and climate settings. This could result in undersampling of particular RTS morphologies and activity levels (e.g., small, lakeside RTS or large inactive RTS landforms) that limit the generalizability of DL frameworks when these are applied outside of the domain area, and may lead to false predictions. As one of the end goals of remotely-sensed detection and delineation is to inform scientists, practitioners, and communities of new RTS locations or RTS growth, false negatives/positives or differing delineations may be artifacts of disparate methods and slump ontology rather than actual change (Van Der Sluijs et al., 2023). These model artifacts can have considerable implications when DL output products are subsequently used for landscape vulnerability assessments such as RTS growth forecasts, or upscaling environmental impacts to larger areas (e.g., carbon/methane).

Compared to other domains, such as everyday imagery with *imagenet* (Deng et al., 2009) or *BigEarthNet* for standard earth observation imagery (Sumbul et al., 2021), there is neither a benchmark set for RTS boundaries nor any intercomparison of RTS labeling results between domain experts to better understand the variability of human-derived training data in the context of RTS mapping efforts using DL. To determine the necessity and properties of such benchmark datasets, we set up an experiment to let domain experts manually label RTS boundaries within satellite imagery and evaluate the degree of agreement or disagreement among them. Such experiments have been conducted for a few other domains such as terrestrial (Guzzetti et al., 2012) or subaqueous (Clare et al., 2019) landslides. The availability of clear instructions, visual examples and professional labeling experience has helped to improve the label quality of biomedical images (Rädsch et al., 2023).

Here we specifically evaluate the consistency and accuracy of labels between twelve international domain experts from various backgrounds, who are all contributors to the International Permafrost Association (IPA) action group on RTS (RTSInTrain). From these results we infer the potential impact on efforts to harmonize and pool pan-Arctic scale training and validation datasets as well as past and future DL-based RTS mapping efforts.

Figure 1: Oblique aerial image of a typical bowl-shaped retrogressive thaw slump (RTS) in NW Canada (67.2588°,-135.2453°). Typical labeling strategies indicated: 1) only highly active regions close to the headwall in green, 2) active areas with wet bare soils including headwall and scar zone in light yellow, 3) RTS footprint including inactive and vegetated parts in orange, and 4) complete RTS including debris tongue in red. Photo: J. Van der Sluijs.

Data and Study Sites

Data

For this experiment we used two study sites, one on the Peel Plateau in Northwestern Canada and a second on the Bykovsky Peninsula close to the Lena Delta in Northeast Siberia (Fig 2). Both sites contain the target landscape features, RTS of different sizes and are located in different landscape settings. These specific sites were chosen as they represent different types of RTS morphologies and landscape settings. As the main data source, we used PlanetScope (Planet Team, 2017) multispectral imagery OrthoTiles, with a spatial resolution of 3.15m per pixel and four spectral bands (Blue, Green, Red, Near-infrared). We used single acquisitions for each site. The scenes were acquired on 2021-08-04 (OrthoTile 4763844_0870513_2021-08-04_2416) for Peel and 2021-07-21 for Bykovsky (OrthoTile 4713120_5272315_2021-07-21_2463) and represent cloud-free and good-quality images. Both scenes were clipped to a size of 2.5x2.5 km, to minimize the labeling efforts and maximize participation of volunteers. To support digitization we added the ArcticDEM (Porter et al., 2018) as well as lower spatial resolution Landsat-8 with 30m and Sentinel-2 with 10m spatial resolution.

158 The Peel site is located on the Peel Plateau at 68.052°N 135.668°W in the Beaufort Delta region of Northwestern
159 Canada (Fig 2a). This region is located in a formerly glaciated area (Kokelj et al., 2017; Segal et al., 2016) with distinct
160 terrain morphology of hills and valleys. The terrain is pronounced with deeply incised valleys and an elevation range
161 of 250 to 500 m. The Peel Plateau is in the tundra-taiga ecotone. Active RTS in this area have a typical round bowl
162 like shape, and a large scar zone with significant volumes of debris, which partially fill the valley downstream (see
163 Fig 2a-I, Figs S1-S2) (Kokelj et al., 2021). In the Beaufort Delta region the location and morphology of active RTS
164 are closely linked to inactive RTS whereby the majority of active thaw slumping processes have occurred in
165 association, or within the footprint, of past disturbances (Van Der Sluijs et al., 2023). This region has been subject to
166 a substantial amount of research (Kokelj et al., 2015, 2017, 2021; Lacelle et al., 2010; Segal et al., 2016) and is well
167 known to the RTS research community.

168 The Bykovsky site is located at 71.881°N 129.293°E on the Bykovsky Peninsula on the Laptev Sea coast southeast of
169 the Lena Delta in Northeastern Siberia (Fig 2b). Permafrost here is dominated by late Pleistocene syngenetic ice-rich
170 Yedoma Ice Complex deposits with a thickness of up to 50 m (Shmelev et al., 2017). In contrast to the Peel site, this
171 area has not been glaciated and the cryostructure of deposits is different and characterized by the large polygonal ice
172 wedges. RTS along this coastline typically have an elongated shape and mostly contain a narrow scar zone along the
173 top slope, known as thermodenudation (Günther et al., 2013), and a stabilized, vegetated zone in the middle and lower
174 slopes (Fig 2b-I, Figs S3-S4). The vegetation is dominated by sparse tundra with differences between undisturbed
175 tundra and recently disturbed areas, such as stabilized RTS scar zones. The terrain is undulating with elevation from
176 sea level to approx. 40 m. This region has been subject to few past studies in the context of slumping and coastal
177 dynamics (Grosse et al., 2005, 2007; Günther et al., 2013; Lantuit et al., 2011).

178

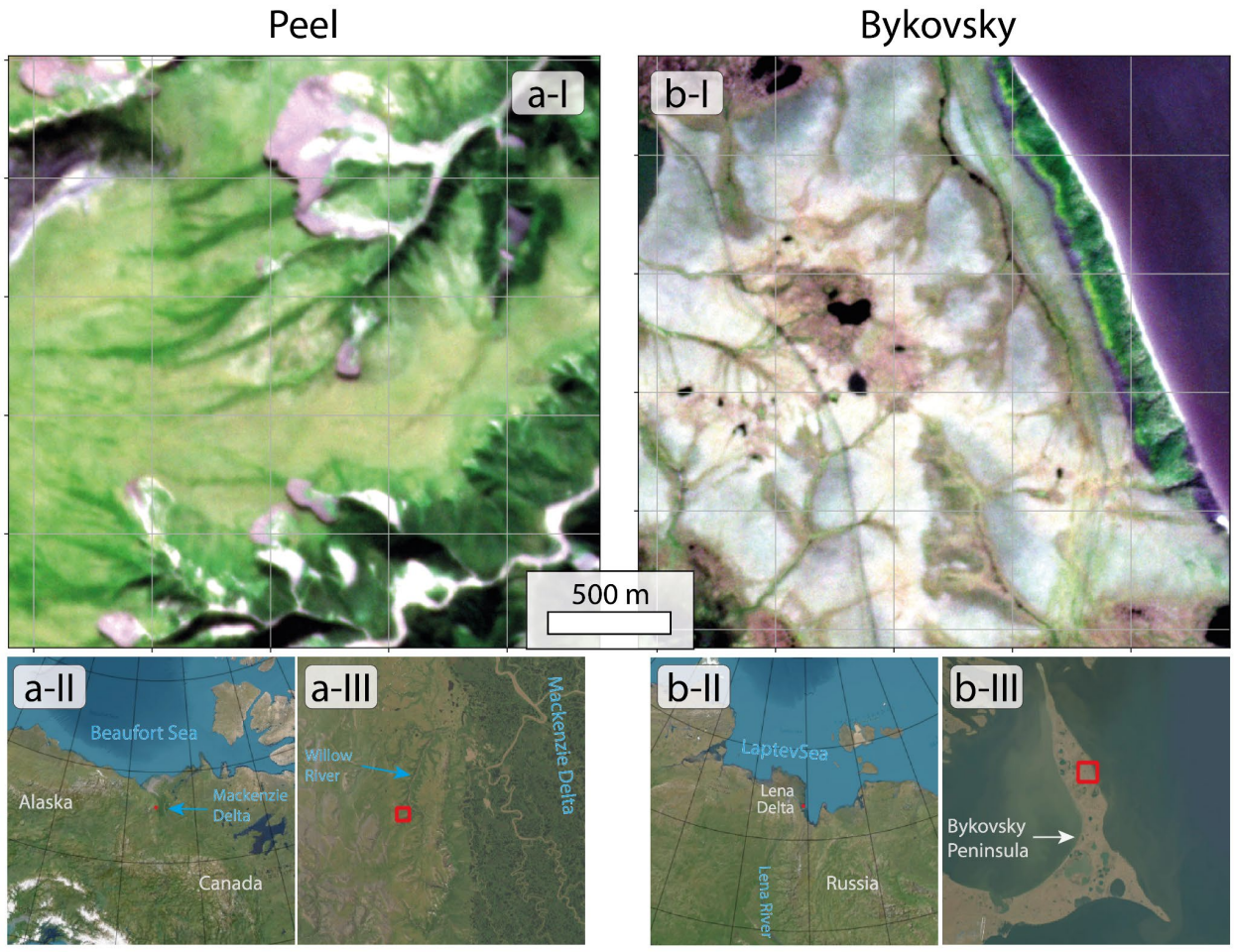

Figure 2: PlanetScope Satellite images of the study sites a) Peel and b) Bykovsky as a real color composite (RGB) with 3.15m nominal spatial resolution, and with overview maps (a/b-II/III) of the locations. Background Map: ESRI Satellite.

Methods

Twelve domain experts, who are all members of the International Permafrost Association (IPA) funded action group on RTS (RTSInTrain), volunteered to participate in this experiment. They have different scientific backgrounds such as geomorphologists, geologists, remote sensing scientists to computer scientists. Furthermore, the current scientific focus varied from geomorphological analysis, to mapping spatial and/or volume changes. Participants come from different countries (Germany, Russia, Canada, USA, China, Switzerland) and have variable experience of RTS fieldwork from none to extensive (see Table S1). The participants' spatial focus and experience also varied strongly from single specific regions such as NW Canada or Tibetan Plateau, to pan-Arctic. For the analysis we anonymized the participants names and assigned each one a random number between 1 and 13 (#01-#13).

Digitization

The participants were requested to manually digitize RTS using a GIS software of their choice and on the provided imagery. The PlanetScope image was supposed to be used as the main labeling source. We further provided the ArcticDEM elevation model and the temporally nearest Landsat and Sentinel-2 scenes. We requested that participants cover each identified RTS by a polygon geometry. We did not provide further instructions to better understand and quantify the individual differences in the absence of specific rulesets (e.g. how to label RTS based on specific geomorphic features).

Evaluation

For quantifying the similarity, we used standard remote sensing and image segmentation metrics, such as Intersection-over-Union, F1, precision and recall. Typically, these metrics are used to validate a prediction versus a ground truth. In our case we validated all unique output combinations against each other. For this we used the digitized vector files and calculated the metrics using the *geopandas* python package. All geospatial data were projected in the respective local UTM zone, Peel in zone 8N (EPSG:32608) and Bykovsky in zone 52N (EPSG:32652).

Results

Peel Plateau

In the Peel Plateau (Fig 3) the participants generally identified the same RTS and digitized similar features. The number of identified individual objects ranged from 7 to 11, with a mode (highest frequency) of 8 and 11 RTS labeled by three people each. The mean ± standard deviation IoU Score is 0.59±0.09 ranging from 0.77 to 0.34 for individual label pairs (Fig 5a). The F1 score is on average 0.74±0.08 and ranges from 0.87 to 0.51. Detailed analysis of each individual combination is provided in Supplementary Table TS2. The best combination was achieved by participants #01 and #03 which happens to be part of the same scientific organization and with internal digitization guidelines in place based on past initiatives (Fig 3c).

In this region differences arise in the digitization of specific features within RTS. All participants digitized the apparently active part close to the headwall with freshly exposed soil and debris. Differences become apparent in the lower parts, most notably the scar zone, which was digitized by almost all participants (11 of 12). The debris tongue and flows were only included by three (#s 05, 09 and 12) of 12 participants. Inactive parts were also treated differently (Fig 3d). Minor differences in label agreement also appear due to slight differences in user created geometries even though digitizing the same feature, e.g. the headwall (Fig 3c). The visual differences in Fig 3b showcase the differences in geomorphological interpretation.

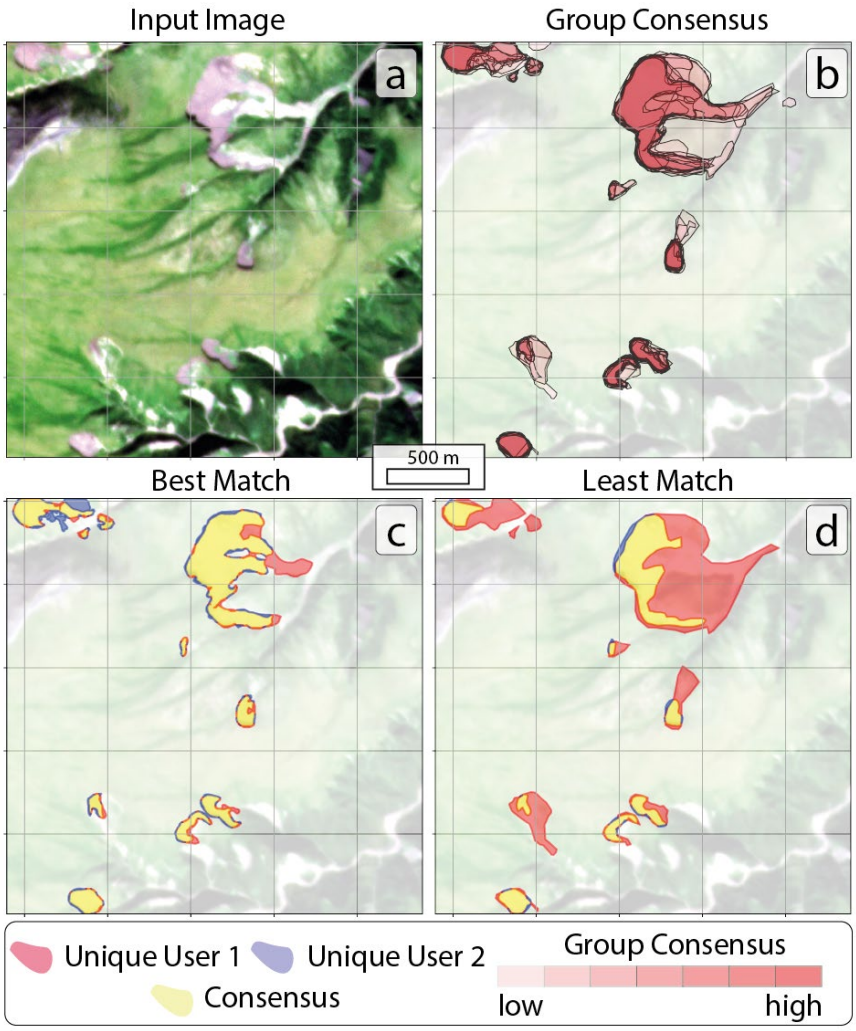

Figure 3: a) PlanetScope satellite image of the study area as a real color composite (RGB), b) the spatial group consensus, the consensus between c) the best matching (users #03 vs. #01), and d) least matching pairs (users #05 vs. #08).

Bykovsky

In Bykovsky (Fig 4) the RTS mapping experiment resulted in considerably different observations than the Peel site with on average less overlap and a lot more variance. The total number of identified individual RTS objects ranged from 1 to 11, with a mode of one large single RTS labeled by four out of 10 people. The mean IoU Score is 0.21±0.31 ranging from 0.92 to 0 (Fig 5b). The F1 score, which is on average 0.26±0.34 ranges from 0.96 to 0. Generally, the results come in three clusters. Cluster 1 recognized the RTS, which are in a terraced shape, and digitized the active scar zone and additionally the stabilized, vegetated parts (Fig 4b-c). The four participants who followed this strategy (#s 04, 05, 09, 10), have high similarity scores/metrics (IoU 0.78-0.92). Similarly, there is a second group (#s 01, 03, 06), who homogeneously digitized only the active scar zones, which results in high similarity within this group (IoU 0.63-0.7). While three of four members of the first group typically have a focus on geomorphology and landform

237 analysis, all members of the second group have a strong focus on mapping RTS (see Tab TS-1). Scores between group
238 1 and 2 are comparably low with IoU from 0.16 to 0.25 due to the large extent of the stabilized zone, although both
239 groups detected the same general features (Fig 4c), which are spatially intersecting. Instead of one large object,
240 common among group 1, members of the second group labeled smaller, but a higher number of individual objects,
241 typically 4 or 5, in one case 11. Detailed analysis of each individual combination is provided in Supplementary Table
242 TS3.

243 The third group (#s 02, 11, 12) digitized some other non-RTS features. Thus, all scores in a comparison to other
244 participants, within this group or each of the other participants, were 0 due to no overlap (Fig 4d). All members of this
245 group only have experience in non Siberian sites but medium to high experience in field work. Two participants (#s
246 07, 08) rejected the digitization task in Bykovsky, due to being unsure if there are any RTS apparent. Both participants
247 have none or little field experience.

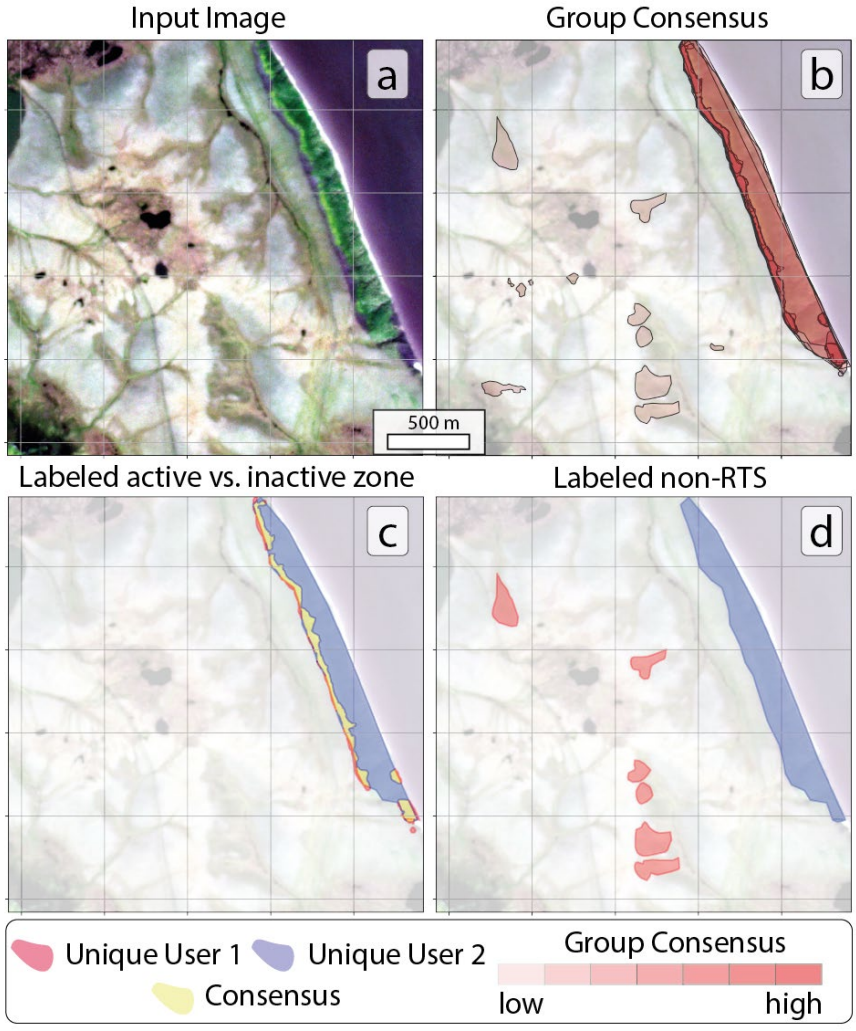

248

249 Figure 4: a) PlanetScope satellite image of the study area as a real color composite (RGB), b) the spatial group
250 consensus, the consensus between c) two users mapping with and without the inactive zone, with a narrow band of

overlap (users #01 vs. #05), and d) least matching pairs with false labeled non-RTS areas (red patches) (users #02 vs. #05).

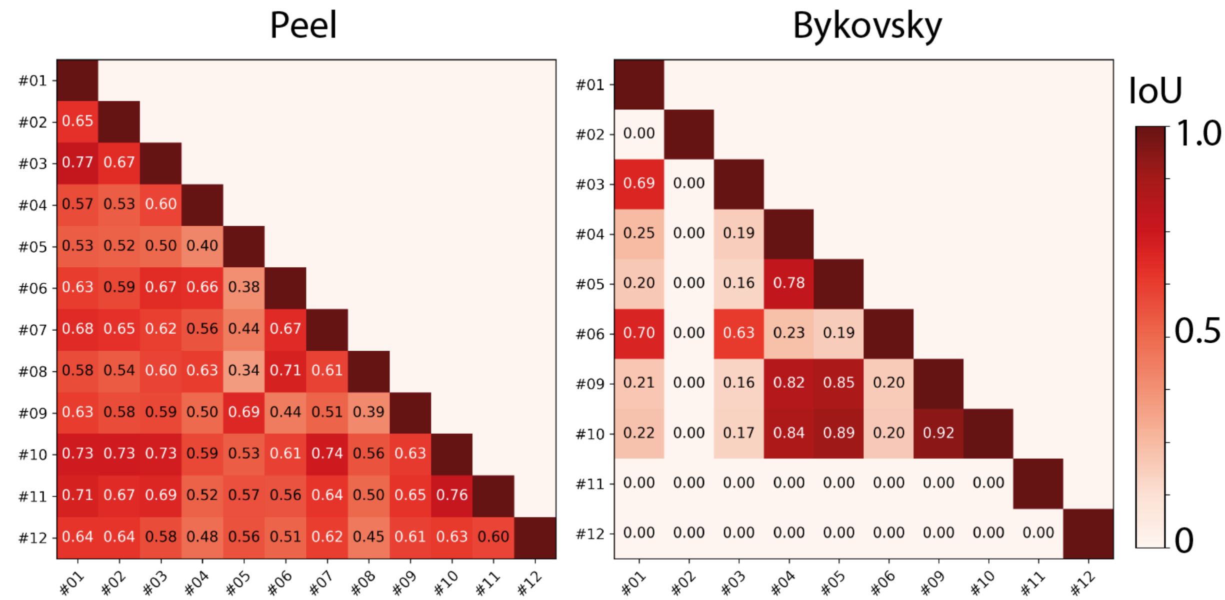

Figure 5: Matrix of Intersection-over-Union (IoU) results for each expert combination in the a) Peel and b) Bykovsky study sites.

Discussion

Landscape settings and RTS types

The labeling experiment highlighted the strong heterogeneity of digitization results of domain experts for RTS. We can therefore conclude that there is a need for a set of guiding principles and standards for consistent RTS labeling across the Arctic, as well as a need for harmonized benchmark datasets. This heterogeneity was seemingly influenced by the shape and geographic setting of the RTS, which became apparent by the differences between both study sites. While the results were more homogenous among all participants in the Peel study site, results in the Bykovsky study site were much more variable with cases of no-overlap at all for some user combinations. This can be attributed to the typical bowl shape of active RTS of the Peel site, a region familiar to most participants due to its extensive literature and visual media showcasing RTS. The Bykovsky site in contrast featured more elongated RTS with a considerable vegetated component in the disturbed footprint, which are typical for Yedoma upland slopes with baydzherakhs (residual thermokarst mounds formed due to the thawing of ice wedges) in Northeastern Siberia and Northwestern America, that are perhaps less well-known. The shape and vegetated component of these RTS are likely considerable drivers of variability among participants as these are more challenging to differentiate with undisturbed tundra. Likewise, their elongated morphology challenges the distinction between neighboring RTS features. In the Russian-language literature there is a specific-term for these elongated-shape RTS, called thermoterrace, there is no such term

in the English-language literature (Nesterova et al., 2024). We therefore hypothesize that the limited detection can be attributed to the lack of regional knowledge and experience of several participants working on coastal RTS, but also stronger exposure to these specific shapes to scientists exposed to Russian terminology.

Local RTS morphology

The second major effect that we observed in this experiment is related to the inclusion or exclusion of certain morphological parts and processes of the mapped RTS. The highly active erosion zone close to the headwall was included with consensus among all participants, with the exception of non-detections in Bykovsky. The consensus decreased with distance from the headwall (see Figs 2c, 3c). While most participants included the non-vegetated scar zone, only few included vegetated parts, such as stabilized parts of RTS. Due to the intentional lack of instructions given, we expected these deviations to some extent. There were two participants previously working together in a team with common labeling guidelines. This pair of researchers produced the highest overlap in the Peel region, and one of the highest in Bykovsky (rank #08) showing the effect of clear instructions in previous work. Providing clear instructions has been also shown to be important in medical labeling exercises (Rädsch et al., 2023). As a second effect, the differences between the participants can be likely attributed to the scientific background and target objectives of the participants. On the one hand, several participants with a focus on geomorphology participated. This group is typically interested in the landform and its local effects and disturbance history, thus including inactive parts and the full debris tongue similar to conventional landslide delineation works (Guzzetti et al., 2012). On the other hand, participants with a strong focus on remotely sensed mapping of RTS typically digitized bare surfaces, which are much easier to distinguish from the (disturbed) vegetated land surface in optical remote sensing data. Furthermore, one participant has a strong remote sensing focus on temporal and episodic volumetric changes, and thus constrained the labeled polygons to the most active area close to the headwall where subsidence or loss of volume is most easily detected. The effect of choice of morphological units on the IoU is so strong, that it may mask an actually good overlap in terms of number of features. Thus including the number of overlapping features is important to identify the object detection performance and accuracy.

More knowledge of local conditions and awareness of landscape history, e.g. inactive RTS, will certainly benefit the labeling performance and confidence. This can be achieved with supporting information, such as photos, geospatial datasets and communication with people with local knowledge. Particularly adding visual examples and the use of hillshaded DEMs can help to improve labeling quality (Rädsch et al., 2023; Van Der Sluijs et al., 2023) especially for people with limited site-specific experience. Assigning labeling confidence, e.g. low, medium, high, and adding further comments, can help to better quantify and understand the label quality, particularly for label data coming from different groups.

In terms of cascading effects of inconsistent labeling, the inclusion of inactive landslide parts by some participants will increase the challenge of remotely-sensed detections of RTS if done automatically, while digitizations of only active RTS will vastly underreport the number (and area) of RTS on a landscape. Thirdly, volumetric changes further away from the immediate headwall zone also constitute important RTS processes, which should not be missed in the calculation of sediment budgets (Kokelj et al., 2021; van der Sluijs et al., 2018). Thus, the results of this work indicated

that differences in RTS labeling will also arise among participants depending on the purpose of the mapping effort, and therefore, what the object needs to portray. These differences are not easily reconciled as an adherence to one labeling standard would limit the usefulness of the labels for specific purposes mentioned. Therefore multiple specific label definitions and target purposes for further application should be provided instead of defining a single standard.

Comparison to published accuracies

The best label combination results with IoU of 0.77 and F1 of 0.87 in the Peel site as well as IoU of 0.92 and F1 of 0.96 in the Bykovsky site, indicate the upper limits of human labeling consistency which we can expect for these sites. The best matching label combinations captured the same features and only minor deviations due to differences in digitization precision. The morphological differences and RTS properties (number, area, shape) between our study sites also highlight the impact of landscape configuration and image content and thus upper envelope of accuracies. Finally, it is expected that spatial resolution has an effect on inter-mapper (human) IoU and F1 scores, as the scores observed in this study (using 3 m PlanetScope) are likely higher than if a similar experiment would be attempted with Sentinel/Landsat imagery (10-30 m), or alternatively, lower than if very high resolution aerial photography and hillshaded LiDAR derived DEMs would be used (Fig. S1).

Previous studies reported maximum IoU values of 0.58 (Nitze et al., 2021), and 0.74 (Yang et al., 2023) or F1 values of 0.73 (Nitze et al., 2021), 0.75-0.85 (Witharana et al., 2022) and 0.85 (Huang et al., 2020). These previous studies typically used calibration and validation data from one or a few participants, thus the maximum IoUs reported reflect the degree to which DL frameworks can mimic the participants' ontological understandings and delineation tendencies. Furthermore, input imagery of different types and spatial resolution complicates the comparison of accuracy metrics. Those DL IoUs are not directly comparable to the human IoU's presented in this work as a range of ontological understandings of RTS are directly compared, rather than against a single source of truth. The experiment's best labeling consistency exceeded all published automated detections, by a slight margin. Generally we can expect human consistency (best combination) as the more or less natural maximum which can be achieved with automated methods. However, we expect that the manual labeling consistency can be further improved with labeling standards in place, which will lead to more consistent and comparable DL mapping results and accuracy assessments.

With a sample of two study sites we unfortunately cannot perform a better uncertainty estimation of the maximum potential performance, yet. However, the strong variation between domain experts shows the drawbacks of human labeling efforts with different ontological understandings or delineation goals and rules. The conclusion from our work underscores the need for caution when pooling calibration and validation data from multiple authors.

Conclusion

Based on our findings there is an obvious need for standards and guidelines for consistent RTS labeling across the Arctic, as well as a need for harmonized benchmark datasets. With clear instructions on which RTS parts to include depending on the mapping objective (e.g., only scar zone, scar zone with inactive/vegetated parts, with or without

debris tongue) human labeling consistency can be enhanced. Adding these instructions with visuals and examples will aid the labeling process, as shown in other scientific domains (Rädsch et al., 2023).

The decision on which parts to include should be carefully based on existing RTS landform and process literature, as few mapping and reporting objectives will be met if RTS descriptions are limited to what can be remotely sensed through automated procedures (i.e., bare surfaces). Furthermore, it is important that RTS benchmarking datasets are carefully reviewed by experienced geomorphologists and ecologists to ensure that a field-based understanding of landform, process, and environmental impact forms the basis on which any future automated detection effort through remote sensing is built.

Creating these guidelines is one of the main deliverables of the RTSInTrain Action group with the International Permafrost Association (IPA). After having specific guidelines we plan to conduct another experiment and compare the results to the initial experiment. Overall, conducting this experiment provided us with a great insight of the RTS labeling process used in past and more current works, and how a diverse group of domain experts thinks about what to label. This will directly lead to the community driven standardization of this process to create consistent labeled datasets, which are essential to train representative DL models.

Acknowledgements

We thank the International Permafrost Association for funding to support in-person meetings and for recognizing this community driven initiative through the IPA Action Group *RTSInTrain*. PlanetScope commercial satellite data were acquired through the HGF AI-CORE Project.

Action group funding by IPA

IN funded by NSF (awards #1927872 #2052107), HGF AI-CORE (also Planet commercial data), ESA CCI+ Permafrost, and BMWK ML4EARTH.

AK was funded by the MSU research program “The cryosphere evolution under climate change and anthropogenic impact” (#121051100164-0)

NN was funded by a DAAD fellowship (Grant #57588368)

MJL was supported by NSF-EnvE (1927772) and NASA-ABoVE (80NSSC22K1254)

AL funded by NSF awards to develop the Permafrost Discovery Gateway (awards #1927872 #2052107)

CW funded by NSF awards to develop the Permafrost Discovery Gateway (award #1927723)

Data

Due to licensing restrictions, we are not allowed to publicly share the commercial PlanetScope input data sources.

Code

https://github.com/initze/RTSIn_experiment (currently private repository) - ask Ingmar (ingmar.nitze@awi.de) to be added

References

Burn, C. R., & Lewkowicz, A. G. (1990). CANADIAN LANDFORM EXAMPLES - 17 RETROGRESSIVE THAW SLUMPS. *The Canadian Geographer/Le Géographe Canadien*, *34*(3), 273–276. https://doi.org/10.1111/j.1541-0064.1990.tb01092.x

Chylek, P., Folland, C., Klett, J. D., Wang, M., Hengartner, N., Lesins, G., & Dubey, M. K. (2022). Annual Mean Arctic Amplification 1970–2020: Observed and Simulated by CMIP6 Climate Models. *Geophysical Research Letters*, *49*(13). https://doi.org/10.1029/2022GL099371

Clare, M., Chaytor, J., Dabson, O., Gamboa, D., Georgiopoulou, A., Eady, H., Hunt, J., Jackson, C., Katz, O., Krastel, S., León, R., Micallef, A., Moernaut, J., Moriconi, R., Moscardelli, L., Mueller, C., Normandeau, A., Patacci, M., Steventon, M., … Jobe, Z. (2019). A consistent global approach for the morphometric characterization of subaqueous landslides. *Geological Society, London, Special Publications*, *477*(1), 455–477. https://doi.org/10.1144/SP477.15

Deng, J., Dong, W., Socher, R., Li, L.-J., Li, K., & Fei-Fei, L. (2009). ImageNet: A large-scale hierarchical image database. *2009 IEEE Conference on Computer Vision and Pattern Recognition*, 248–255. https://doi.org/10.1109/CVPR.2009.5206848

Grosse, G., Schirrmeister, L., Kunitsky, V. V., & Hubberten, H.-W. (2005). The use of CORONA images in remote sensing of periglacial geomorphology: An illustration from the NE Siberian coast. *Permafrost and Periglacial Processes*, *16*(2), 163–172. https://doi.org/10.1002/ppp.509

Grosse, G., Schirrmeister, L., Siegert, C., Kunitsky, V. V., Slagoda, E. A., Andreev, A. A., & Dereviagyn, A. Y. (2007). Geological and geomorphological evolution of a sedimentary periglacial landscape in Northeast Siberia during the Late Quaternary. *Geomorphology*, *86*(1–2), 25–51. https://doi.org/10.1016/j.geomorph.2006.08.005

Günther, F., Overduin, P. P., Sandakov, A. V., Grosse, G., & Grigoriev, M. N. (2013). Short- and long-term thermo-erosion of ice-rich permafrost coasts in the Laptev Sea region. *Biogeosciences*, *10*(6), 4297–4318.

https://doi.org/10.5194/bg-10-4297-2013

Guzzetti, F., Mondini, A. C., Cardinali, M., Fiorucci, F., Santangelo, M., & Chang, K.-T. (2012). Landslide inventory maps: New tools for an old problem. *Earth-Science Reviews*, *112*(1–2), 42–66. https://doi.org/10.1016/j.earscirev.2012.02.001

Huang, L., Liu, L., Luo, J., Lin, Z., & Niu, F. (2021). Automatically quantifying evolution of retrogressive thaw slumps in Beiluhe (Tibetan Plateau) from multi-temporal CubeSat images. *International Journal of Applied Earth Observation and Geoinformation*, *102*, 102399. https://doi.org/10.1016/j.jag.2021.102399

Huang, L., Luo, J., Lin, Z., Niu, F., & Liu, L. (2020). Using deep learning to map retrogressive thaw slumps in the Beiluhe region (Tibetan Plateau) from CubeSat images. *Remote Sensing of Environment*, *237*, 111534. https://doi.org/10.1016/j.rse.2019.111534

Huang, L., Willis, M. J., Li, G., Lantz, T. C., Schaefer, K., Wig, E., Cao, G., & Tiampo, K. F. (2023). Identifying active retrogressive thaw slumps from ArcticDEM. *ISPRS Journal of Photogrammetry and Remote Sensing*, *205*, 301–316. https://doi.org/10.1016/j.isprsjprs.2023.10.008

Kerfoot, D. E. (1969). *The geomorphology and permafrost conditions of Garry Island, N.W.T.* https://doi.org/10.14288/1.0102152

Kokelj, S. V., Kokoszka, J., van der Sluijs, J., Rudy, A. C. A., Tunnicliffe, J., Shakil, S., Tank, S. E., & Zolkos, S. (2021). Thaw-driven mass wasting couples slopes with downstream systems, and effects propagate through Arctic drainage networks. *The Cryosphere*, *15*(7), 3059–3081. https://doi.org/10.5194/tc-15-3059-2021

Kokelj, S. V., Lantz, T. C., Tunnicliffe, J., Segal, R., & Lacelle, D. (2017). Climate-driven thaw of permafrost preserved glacial landscapes, northwestern Canada. *Geology*, *45*(4), 371–374. https://doi.org/10.1130/G38626.1

Kokelj, S. V., Tunnicliffe, J., Lacelle, D., Lantz, T. C., Chin, K. S., & Fraser, R. (2015). Increased precipitation drives mega slump development and destabilization of ice-rich permafrost terrain, northwestern Canada. *Global and Planetary Change*, *129*, 56–68. https://doi.org/10.1016/j.gloplacha.2015.02.008

Lacelle, D., Bjornson, J., & Lauriol, B. (2010). Climatic and geomorphic factors affecting contemporary (1950-2004) activity of retrogressive thaw slumps on the Aklavik Plateau, Richardson Mountains, NWT, Canada: Climatic and Geomorphic Factors affecting Thaw Slump Activity. *Permafrost and Periglacial Processes*, *21*(1), 1–15. https://doi.org/10.1002/ppp.666

Lantuit, H., Atkinson, D., Paul Overduin, P., Grigoriev, M., Rachold, V., Grosse, G., & Hubberten, H.-W. (2011). Coastal erosion dynamics on the permafrost-dominated Bykovsky Peninsula, north Siberia, 1951–2006. *Polar Research*, *30*(1), 7341. https://doi.org/10.3402/polar.v30i0.7341

Lantz, T. C., & Kokelj, S. V. (2008). Increasing rates of retrogressive thaw slump activity in the Mackenzie Delta region, N.W.T., Canada. *Geophysical Research Letters*, *35*(6), L06502. https://doi.org/10.1029/2007GL032433

Lewkowicz, A. G., & Way, R. G. (2019). Extremes of summer climate trigger thousands of thermokarst landslides in a High Arctic environment. *Nature Communications*, *10*(1), Article 1. https://doi.org/10.1038/s41467-019-09314-7

Ma, L., Liu, Y., Zhang, X., Ye, Y., Yin, G., & Johnson, B. A. (2019). Deep learning in remote sensing applications: A meta-analysis and review. *ISPRS Journal of Photogrammetry and Remote Sensing*, *152*, 166–177. https://doi.org/10.1016/j.isprsjprs.2019.04.015

Mackay, J. R. (1966). Segregated epigenetic ice and slumps in permafrost, Mackenzie Delta area, NWT. *Geographical Bulletin*, *8*, 59–80.

Meredith, M., Sommerkorn, M., Cassotta, S., Derksen, C., Ekaykin, A., Hollowed, A., Kofinas, G., Mackintosh, A., Melbourne-Thomas, J., & Muelbert, M. M. C. (2019). *Polar Regions. Chapter 3, IPCC Special Report on the Ocean and Cryosphere in a Changing Climate*.

Nesterova, N., Leibman, M., Kizyakov, A., Lantuit, H., Tarasevich, I., Nitze, I., Veremeeva, A., & Grosse, G. (2024). *Review article: Retrogressive thaw slump theory and terminology* [Preprint]. Frozen ground/Geomorphology. https://doi.org/10.5194/egusphere-2023-2914

Nitze, I., Grosse, G., Jones, B. M., Romanovsky, V. E., & Boike, J. (2018). Remote sensing quantifies widespread abundance of permafrost region disturbances across the Arctic and Subarctic. *Nature Communications*, *9*(1), 5423. https://doi.org/10.1038/s41467-018-07663-3

Nitze, I., Heidler, K., Barth, S., & Grosse, G. (2021). Developing and Testing a Deep Learning Approach for Mapping Retrogressive Thaw Slumps. *Remote Sensing*, *13*(21). https://doi.org/10.3390/rs13214294

Planet Team. (2017). *Planet Application Program Interface: In Space for Life on Earth*. Planet. https://api.planet.com

Plank, B. (2022). *The "Problem" of Human Label Variation: On Ground Truth in Data, Modeling and Evaluation*.

https://doi.org/10.48550/ARXIV.2211.02570

Porter, C., Morin, P., Howat, I., Noh, M.-J., Bates, B., Peterman, K., Keesey, S., Schlenk, M., Gardiner, J., Tomko, K., Willis, M., Kelleher, C., Cloutier, M., Husby, E., Foga, S., Nakamura, H., Platson, M., Wethington, M., Williamson, C., … Bojesen, M. (2018). *ArcticDEM* [dataset]. Harvard Dataverse. https://doi.org/10.7910/DVN/OHHUKH

Rädsch, T., Reinke, A., Weru, V., Tizabi, M. D., Schreck, N., Kavur, A. E., Pekdemir, B., Roß, T., Kopp-Schneider, A., & Maier-Hein, L. (2023). Labelling instructions matter in biomedical image analysis. *Nature Machine Intelligence*, *5*(3), 273–283. https://doi.org/10.1038/s42256-023-00625-5

Runge, A., Nitze, I., & Grosse, G. (2022). Remote sensing annual dynamics of rapid permafrost thaw disturbances with LandTrendr. *Remote Sensing of Environment*, *268*, 112752. https://doi.org/10.1016/j.rse.2021.112752

Segal, R. A., Lantz, T. C., & Kokelj, S. V. (2016). Acceleration of thaw slump activity in glaciated landscapes of the Western Canadian Arctic. *Environmental Research Letters*, *11*(3), 034025. https://doi.org/10.1088/1748-9326/11/3/034025

Serreze, M. C., & Barry, R. G. (2011). Processes and impacts of Arctic amplification: A research synthesis. *Global and Planetary Change*, *77*(1), 85–96. https://doi.org/10.1016/j.gloplacha.2011.03.004

Shmelev, D., Veremeeva, A., Kraev, G., Kholodov, A., Spencer, R. G. M., Walker, W. S., & Rivkina, E. (2017). Estimation and Sensitivity of Carbon Storage in Permafrost of North-Eastern Yakutia: Estimation and sensitivity of carbon storage. *Permafrost and Periglacial Processes*, *28*(2), 379–390. https://doi.org/10.1002/ppp.1933

Sumbul, G., De Wall, A., Kreuziger, T., Marcelino, F., Costa, H., Benevides, P., Caetano, M., Demir, B., & Markl, V. (2021). BigEarthNet-MM: A Large-Scale, Multimodal, Multilabel Benchmark Archive for Remote Sensing Image Classification and Retrieval [Software and Data Sets]. *IEEE Geoscience and Remote Sensing Magazine*, *9*(3), 174–180. https://doi.org/10.1109/MGRS.2021.3089174

Swanson, D., & Nolan, M. (2018). Growth of Retrogressive Thaw Slumps in the Noatak Valley, Alaska, 2010–2016, Measured by Airborne Photogrammetry. *Remote Sensing*, *10*(7), 983. https://doi.org/10.3390/rs10070983

van der Sluijs, J., Kokelj, S., Fraser, R., Tunnicliffe, J., & Lacelle, D. (2018). Permafrost Terrain Dynamics and Infrastructure Impacts Revealed by UAV Photogrammetry and Thermal Imaging. *Remote Sensing*, *10*(11),

1734. https://doi.org/10.3390/rs10111734

Van Der Sluijs, J., Kokelj, S. V., & Tunnicliffe, J. F. (2023). Allometric scaling of retrogressive thaw slumps. *The Cryosphere*, *17*(11), 4511–4533. https://doi.org/10.5194/tc-17-4511-2023

Ward Jones, M. K., Pollard, W. H., & Jones, B. M. (2019). Rapid initialization of retrogressive thaw slumps in the Canadian high Arctic and their response to climate and terrain factors. *Environmental Research Letters*, *14*(5), 055006. https://doi.org/10.1088/1748-9326/ab12fd

Witharana, C., Udawalpola, M. R., Liljedahl, A. K., Jones, M. K. W., Jones, B. M., Hasan, A., Joshi, D., & Manos, E. (2022). Automated Detection of Retrogressive Thaw Slumps in the High Arctic Using High-Resolution Satellite Imagery. *Remote Sensing*, *14*(17), 4132. https://doi.org/10.3390/rs14174132

Wulder, M. A., Roy, D. P., Radeloff, V. C., Loveland, T. R., Anderson, M. C., Johnson, D. M., Healey, S., Zhu, Z., Scambos, T. A., Pahlevan, N., Hansen, M., Gorelick, N., Crawford, C. J., Masek, J. G., Hermosilla, T., White, J. C., Belward, A. S., Schaaf, C., Woodcock, C. E., … Cook, B. D. (2022). Fifty years of Landsat science and impacts. *Remote Sensing of Environment*, *280*, 113195. https://doi.org/10.1016/j.rse.2022.113195

Xia, Z., Huang, L., Fan, C., Jia, S., Lin, Z., Liu, L., Luo, J., Niu, F., & Zhang, T. (2022). *Retrogressive thaw slumps along the Qinghai-Tibet Engineering Corridor: A comprehensive inventory and their distribution characteristics* [Preprint]. Cryosphere – Permafrost. https://doi.org/10.5194/essd-2021-439

Yang, Y., Rogers, B. M., Fiske, G., Watts, J., Potter, S., Windholz, T., Mullen, A., Nitze, I., & Natali, S. M. (2023). Mapping retrogressive thaw slumps using deep neural networks. *Remote Sensing of Environment*, *288*, 113495. https://doi.org/10.1016/j.rse.2023.113495

Zhu, X. X., Tuia, D., Mou, L., Xia, G.-S., Zhang, L., Xu, F., & Fraundorfer, F. (2017). Deep Learning in Remote Sensing: A Comprehensive Review and List of Resources. *IEEE Geoscience and Remote Sensing Magazine*, *5*(4), 8–36. https://doi.org/10.1109/MGRS.2017.2762307

Supplement to:

A labeling intercomparison of retrogressive thaw slumps by a diverse group of domain experts

Nitze et al.

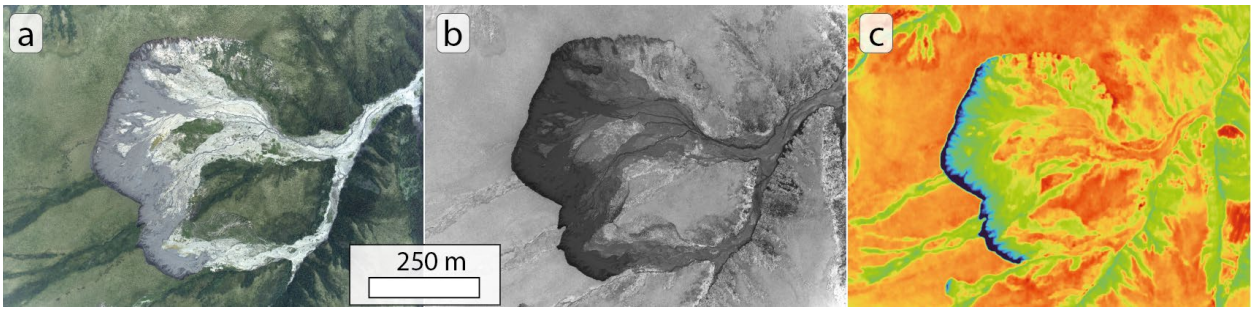

Figure S1: Aerial imagery of the large RTS in the Peel site in a) Real-color, b) Near-infrared, and c) thermal-infrared, acquired on 2023-07-07. Imagery acquired during AWI PermaX23 aerial imaging campaign.

Figure S2: Oblique aerial image of the large RTS in the Peel site, acquired on 2023-07-07. Imagery acquired during AWI PermaX23 aerial imaging campaign. Photo: I.Nitze

Figure S3: Upper part of the coastal RTS with vegetation cover in the stabilized part, complex of vegetation and bare soil in the scar zone and ice-rich headwall on Bykovsky Peninsula in the study area taken in Summer 2016. Photo A.Kizyakov. See persons for scale.

Figure S4: RTS base with visible vegetation in stabilized parts and headwall with overhanging peat cover on Bykovsky Peninsula in the study area taken on 2014-08-21. Person for scale. Photo I.Nitze

SUPPLEMENTARY TABLE TS1

LIST OF PARTICIPATING EXPERTS AND THEIR SCIENTIFIC BACKGROUND, FIELDWORK EXPERIENCE AND MAIN OBJECTIVES

creator_id	Scientific Background (Topic)	Field Experience	Spatial focus regions	Thematic Focus	Affiliation Region
#01	Physical Geography, Remote Sensing, Geoinformatics	medium	Arctic	Mapping (2D)	Central Europe
#02	Earth Science, Geoinformatics	medium	Tibetan Plateau, Arctic	Mapping (2D)	North America / East Asia
#03	Physical Geography	little	Russia/Siberia	Mapping (2D)	Central Europe
#04	Physical Geography	high	Russia/Siberia	Geomorphology	Russia
#05	Physical Geography	medium	Russia/Siberia	Geomorphology	Central Europe / Russia
#06	Earth Science, Geospatial Data Science, Remote Sensing	none	Arctic	Mapping (2D)	North America
#07	Remote Sensing	little	Tibetan Plateau	Mapping (2D)	East Asia
#08	Physics	none	Arctic	Mapping (3D)	Central Europe

#09	Physical Geography, Remote Sensing	high	Canada	Geomorph. + Mapping	North America
#10	Georaphy, Earth Observation and Geo-Information Science	little	Russia/Siberia	Mapping (2D)	Central Europe
#11	Ecology and Remote Sensing	high	Alaska	Geomorphology	North America
#12	Physical Geography	high	Canada	Geomorphology	North America

SUPPLEMENTARY TABLE TS-2

OVERVIEW OF RESULTS FOR ALL EXPERT LABELING COMBINATIONS IN THE PEEL STUDY SITE

Link: Peel_correlation_summary.html (formatted table, please download and open in browser)

SUPPLEMENTARY TABLE TS-3

OVERVIEW OF RESULTS FOR ALL EXPERT LABELING COMBINATIONS IN THE BYKOVSKY STUDY SITE

Link: Bykovsky_correlation_summary.html (formatted table, please download and open in browser)

Zipped archives of data analysis output (figures)

Peel (308MB):
https://drive.google.com/file/d/1I0qo08rs23zMf9MKcPORxA34hERq_Q0f/view?usp=sharing
Bykovsky (240MB):
https://drive.google.com/file/d/1Hqkch9ZOuurVlT1shQ6_nmDkaY55W6Wa/view?usp=sharing

Code for data analysis and figures

https://github.com/initze/RTSIn_experiment